



# Residual chlorine prevents full densification of 3 mol% yttria-stabilized zirconia ceramics during ultrafast high-temperature sintering (UHS)

Vladimír Prajzler<sup>a,b,\*</sup>, Zonghao Guo<sup>b</sup>, Stanislav Pruša<sup>a,c</sup>, Richard I. Todd<sup>b</sup>

<sup>a</sup> Brno University of Technology, CEITEC, Purkyňova 123, Brno 612 00, Czech Republic

<sup>b</sup> University of Oxford, Department of Materials, Parks Road, Oxford OX1 3PH, United Kingdom

<sup>c</sup> Brno University of Technology, Faculty of Mechanical Engineering, Technická 2896/2, Brno 616 69, Czech Republic

## ARTICLE INFO

### Keywords:

Zirconia  
Ultrafast high-temperature sintering  
Densification  
Residual chlorine  
Shell-like structure  
LEIS

## ABSTRACT

As-received commercially available 3 mol% yttria-stabilized zirconia (3YSZ) powders often contain residual chlorine, an impurity from powder synthesis, which can negatively impact densification during sintering. This is because the ultra-fast heating rate results in rapid pore closure and entrapment of chlorine species in the sintered samples. This study shows that residual chlorine, detected using Low Energy Ion Scattering (LEIS), significantly hindered the densification of binderless 3YSZ during ultrafast high-temperature sintering (UHS), resulting in only 87 % of theoretical density. Although all as-received 3YSZ powders contained chlorine in comparable amounts, powders with added binder allowed the chlorine to be removed at low temperature, resulting in high sintered densities. This finding shows that the use of appropriate 3YSZ powder with zero or low levels of residual chlorine can avoid the necessity of chlorine elimination through pre-sintering at 1000 °C, which significantly enhances the effectiveness of the UHS method.

## 1. Introduction

Modern sintering methods often use rapid heating rates, several orders of magnitude higher than conventional sintering [1]. This is because of several practical reasons: the acceleration of the sintering process reduces time and energy requirements, and the effect of rapid heating on the microstructure evolution has been described as positive in several studies [2–4]. Rapid heating in ceramic science has its origins in the last century, where it became an important aspect of techniques such as fast firing, microwave sintering, and spark plasma sintering. Flash sintering further explored the benefits of rapid heating rates during the last decades, and recently, Wang et al. [5] proposed a promising sintering technique named ultrafast high-temperature sintering (UHS). The UHS setup is relatively simple. A powder compact is placed within a split graphite felt that is heated up to the sintering temperature in a few seconds by the application of electric current.

The UHS of yttria-stabilized zirconia (YSZ) has been the subject of many studies [4–8], with the common conclusion that YSZ powders can be fully densified in  $\leq 60$  s [6–8]. Here it is important to note that a high density of over 99 %TD was often attained in studies that pre-sintered YSZ green bodies in a muffle furnace at 1000 °C for 60 min before UHS [6–8]. It is evident that the pre-sintering cycle increased the overall

fabrication time and energy consumption. The justification for the pre-sintering was the necessity to remove entrapped gases, however, no further references and discussion on the origin and nature of the entrapped gases were included in references [6–8]. Moreover, the studies which did not use this pre-sintering cycle reported notably lower final densities: around 97 % [4], and 95 % [5].

We assume that the entrapped gases mentioned in references [6–8] are chloride-based species that are developed during a reaction of residual chlorine (a trace impurity from powder synthesis) with YSZ. Our assumption is based on the well-known fact that the entrapped chlorine negatively affects the densification of YSZ ceramics during fast firing and microwave sintering [9–11]. Due to the fast heating, the residual chlorine does not have enough time to leave the powder compact before the pores are closed, and thus, becomes trapped inside the sintered body and prevents further densification [9–11]. The chlorine impurities were also found to be responsible for poor densification of YSZ ceramics during flash sintering [12], which is in some ways a very different process (inside out heating, electric current interactions with sample, colder surrounding atmosphere etc.). Given the increasing interest in UHS as a scalable, ultrafast sintering technique, it is critical to determine whether residual chlorine imposes similar densification limits.

This study investigates the effect of residual chlorine on the

\* Corresponding author at: Brno University of Technology, CEITEC, Purkyňova 123, Brno 612 00, Czech Republic.

E-mail address: [vladimir.prajzler@ceitec.vutbr.cz](mailto:vladimir.prajzler@ceitec.vutbr.cz) (V. Prajzler).

<https://doi.org/10.1016/j.jeurceramsoc.2025.117709>

Received 6 May 2025; Received in revised form 15 July 2025; Accepted 22 July 2025

Available online 23 July 2025

0955-2219/© 2025 The Authors. Published by Elsevier Ltd. This is an open access article under the CC BY license (<http://creativecommons.org/licenses/by/4.0/>).

densification of commercially available 3 mol% yttria-stabilized zirconia (3YSZ) ceramics during UHS. Given the similarity between fast firing and UHS processes – both of which employ rapid heating rates without external pressure – it is reasonable to assume that residual chlorine will also impair the densification of YSZ during UHS as well. However, there are still differences between the two processes: (1) fast firing involves no electric current through the sample, whereas UHS may involve a small current, depending on the specific material and setup, (2) fast firing of 3YSZ is typically conducted in air, while UHS is usually performed under an inert atmosphere, (3) thermal radiation from heating elements is typically the dominant heat transfer mechanism in both processes, particularly at high temperatures where the radiative heat flux becomes significant, but specimens in UHS setup may experience heat faster due to direct contact with graphite felt. Despite these differences, our results presented and discussed in this article confirm the assumption that residual chlorine is an issue during UHS and give a simple conclusion: 3YSZ powder compacts containing a substantial amount of residual chlorine during UHS will densify poorly, while powder compacts with zero or low levels of residual chlorine will densify well.

## 2. Experimental

### 2.1. Sample preparation

Four powders of commercially available 3 mol% yttria-stabilized zirconia were investigated in this study: TZ-3Y, TZ-3Y-E, TZ-3YB, and TZ-3YB-E (Tosoh Corp., Japan), see Table 1. Two of them were binderless: TZ-3Y, TZ-3Y-E, and the other two contained about 3.5 wt% of organic binder: TZ-3YB, TZ-3YB-E. The differences between TZ-3Y and TZ-3Y-E, as well as between TZ-3YB and TZ-3YB-E, lie in alumina doping. The “E” variants contain about 0.25 wt% of Al<sub>2</sub>O<sub>3</sub>. The as-received powders were uniaxially pressed into disc-shaped specimens at 60 MPa using a stainless-steel die, followed by cold isostatic pressing at 256 MPa. The green bodies had dimensions of 7.7 mm in diameter and 1.5 mm in thickness. All specimens were first heated to 600 °C at 600 °C/h and held for 1 h to remove the organic binder and impurities.

### 2.2. Ultrafast high-temperature sintering

The UHS was performed in an inert argon atmosphere using a prototype sintering apparatus. Green bodies were inserted in split graphite felt suspended between copper electrodes in a glass container, as described in detail elsewhere [13]. The container was filled with flowing argon and the graphite felt was heated via a DC power supply (EA-PS 9360–15, 1500 W, Electro-Automatik, Viersen, Germany) in constant power mode. The UHS was conducted using a two-step heating process. The felt was first heated to 780 ± 15 °C and held there for 90 s. The purpose of the pre-heat was to remove sample moisture and reduce the thermal stress during rapid heating to the sintering temperature so that cracking of the sample was avoided. The power was then increased to heat the felt to the designated sintering temperature in the range 900 – 1800 °C and held for 60 s. The power ramp was conducted at the maximum rate the power supply permits, resulting in a sample heating rate of around 120 – 140 °C/s. The power supply was then turned off, allowing a fast cool down. As a reference, one 3Y sample was sintered conventionally in air, using a box furnace. The heating rate was

5 °C/min up to 1500 °C with 30 min dwell time.

The temperature calibration of the UHS setup was performed by using a partially hollow alumina disc, inserted in a graphite felt slit, which acted as shielding for a R-type thermocouple (Omega P13R-001, 0.125 mm diameter wires). The temperatures for different power levels were measured. To verify thermocouple temperature measurements, pure metal wires (Zn, Cu, Fe, Ni, Pt, ≥ 99.9 % pure, 0.25 mm, Sigma Aldrich) were placed into the partially hollow alumina disc, which was then heated inside the felt slit as in the case of thermocouple calibration. The lowest power level at which each metallic wire melted was considered to represent the melting temperature of the respective metal. More details on calibration can be found in work [13].

### 2.3. Sample characterization

The relative densities of the sintered samples were measured based on the Archimedes technique (EN 623–2) using a theoretical density of 6.05 g/cm<sup>3</sup>. The microstructure was characterized by scanning electron microscopy (SEM, Verios 460 L, FEI) using polished and thermally etched cross-sections. The steps taken during sample preparation for SEM imaging are schematically displayed in Fig. 1. The etching temperature was 1250 °C for 15 min. SEM images were taken from near the surface and from the core area. The grain size was measured using line intercept method and then multiplied by factor of 1.56 [14]. The amount of residual chlorine in sintered samples was studied by High-Sensitivity Low Energy Ion Scattering (LEIS) analysis (Qtac 100, ION-TOF GmbH, Germany) by comparing Cl peak intensities. It is an extremely surface-sensitive technique that enables elemental characterization of the outermost atomic layer [15]. The measurement was performed in the analytical chamber of the LEIS instrument at room temperature with a base pressure of 8 × 10<sup>−9</sup> Pa. The analysed area was 1 mm<sup>2</sup> at the fracture surface of the sintered samples. All spectra were measured after a light sputtering by helium (2 × 10<sup>15</sup> He/cm<sup>2</sup>). Four separate scans were performed at different locations on the fracture surface of each sample.

## 3. Results and discussion

The relative densities of UHS samples are shown in Fig. 2. The densification started around the same temperature for all investigated powder batches. This is because of the same particle size and nearly identical chemical composition. Then the densification became slightly accelerated for alumina-containing “E” grade specimens (3YE, 3YBE samples). This is a well-documented phenomenon in 3YSZ ceramics, caused by a decrease in the activation energy for diffusion in the early stages of sintering as a result of the Al<sub>2</sub>O<sub>3</sub> additions in these powders [16]. Nearly fully dense specimens were obtained with binder-containing powders (3YB, 3YBE samples). In contrast, the binderless powders (3Y, 3YE samples) densified poorly. The highest densities of 3Y and 3YE samples were only 86.9 and 87.0 %TD when sintered at ~1650 °C.

Here it is necessary to emphasize that the poor densification of 3Y and 3YE samples manifested by non-densifying porous cores (Fig. 3a, c) was not caused by the external heating alone, as all the samples had the same geometry and size, as well as the same mass and thermal conductivity. The results of more detailed analysis of average grain size are shown in Fig. 4. Local grain size variations across the sample surface

**Table 1**

3YSZ powder grades used for green body preparation, specific surface area and chemical composition were provided in material data sheets by Tosoh Corp., Japan.

Sample name	Powder	Powder batch number	Specific surface area (m <sup>2</sup> /g)	Chemical composition (wt%)				
				Y <sub>2</sub> O <sub>3</sub>	Al <sub>2</sub> O <sub>3</sub>	SiO <sub>2</sub>	Fe <sub>2</sub> O <sub>3</sub>	Na <sub>2</sub> O
3Y	TZ–3Y	Z304609P	16 ± 3	5.26	0.005	0.002	0.002	0.018
3YB	TZ–3YB	Z300889B	16 ± 3	5.21	0.005	0.002	0.002	0.019
3YE	TZ–3Y-E	Z307071P	16 ± 3	5.29	0.249	0.002	0.003	0.022
3YBE	TZ–3YB-E	Z300453B	16 ± 3	5.22	0.254	0.002	0.003	0.024

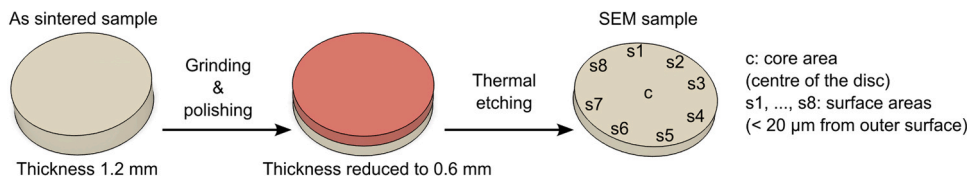


Fig. 1. Schematic illustration of steps taken during SEM sample preparation.

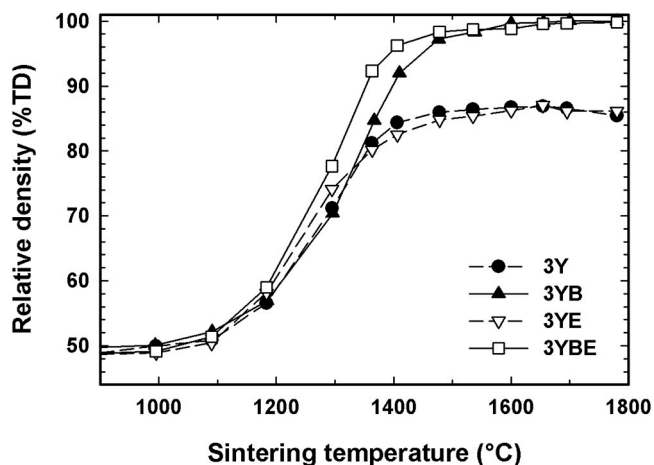


Fig. 2. Relative densities of ultra-fast sintered samples.

were attributed to anisotropic thermal exposure during UHS. Due to the heating geometry and sample placement within the graphite felt, different surface regions may experience significantly different temperatures, as demonstrated by Mishra et al. [17]. This leads to grain growth asymmetries even in nominally uniform samples. More importantly, all samples exhibited similar gradient, so we can rule out these asymmetries as origin of lower final densities observed in some UHS samples.

The poor densification behaviour was previously reported for microwave sintered YSZ [9], fast fired YSZ [9–11,18], and recently also for flash sintered YSZ [12]. All these techniques utilize rapid heating rates, similar to the UHS in this study. These studies attributed poor densification to the entrapment of residual chlorine in the rapidly closing pores and provided evidence of residual chlorine in as-received YSZ powders [9–12]. The residual chlorine in YSZ was attributed to the use of chloride precursors ( $ZrCl_4$  and  $YCl_3$ ) during powder synthesis. It has also been disproved that poor densification is caused by low starting density and/or density gradients in green bodies [10]. As shown in the [Supplementary Materials](#), we verified this statement by preparing green bodies with a wider range of starting densities. The 3YB green bodies always densified better than 3Y green bodies, even when pressed at lower pressures (having lower green body density than 3Y), so lower green density is not the origin of poor densification behaviour.

Most previous reports also pointed out the strong binding of the chlorine to the YSZ particles, resulting in a relatively high evaporation temperature of around 975 °C [10,11,19]. This represents a temperature close to the onset of densification of nanocrystalline 3YSZ, and thus, one can assume that the evaporating chlorine species are immediately trapped in closing pores during ultrafast heating. There is an agreement that the trapped residual chlorine volatilises as  $ZrCl_4$  [10,11] which then alters matter transport from densifying solid-state diffusion towards non-densifying vapour transport as described in reference [20]. The surface region, where the  $ZrCl_4$  can escape, eventually densifies to nearly full density, creating a characteristic shell-like structure [10–12], with a non-densifying porous core of the specimen. This shell-like surface phenomenon was observed in our ultrafast sintered 3Y and 3YE samples (Fig. 3).

It is also known that once the remaining pores are isolated from the surrounding atmosphere by an airtight surface shell, the increasing  $ZrCl_4$  gas pressure can even lead to a decrease in the relative density with increasing sintering temperature and/or sintering time, as shown in references [10,11]. As displayed in Fig. 2, this occurred in our poorly densified 3Y and 3YE specimens as well; the relative density reached a peak at ~1650 °C and then slowly decreased with increasing sintering temperature.

We used the same powder batches as in the study [11] where all the examined 3YSZ powder grades contained approximately 0.07 wt% of chlorine in the as-received state. The work [11] sintered the same powder grades by a fast firing technique with comparable outcomes: binder-containing YSZ densified well, while binderless YSZ densified poorly. Despite comparable chlorine amounts in as-received powders, the different densification behaviour among the samples was attributed to a chlorine reduction in binder-containing bodies. It was shown that a physical and chemical processes during binder burnout resulted in the release of residual chlorine around 400 °C (Figure 6 in Ref. [11]). This behaviour was affirmed in work [12]; no chlorine was detected in binder-containing bodies after heating at 900 °C, while binderless bodies still contained approximately the same amount of chlorine as in the as-received state. We assume that chlorine “de-contamination” during binder burnout in binder-containing bodies occurred also in this study as we used the same powder batch and observed the same densification behaviour as in previous studies, where the binder-containing powders densified without any issues.

The remaining question as to whether residual chlorine was present in the poorly densified 3YSZ samples during sintering was answered by the LEIS analysis. Fig. 5 shows LEIS spectra of four samples UHSed at 1406 °C ( $3Y^{UHS}$ ,  $3YB^{UHS}$ ,  $3YE^{UHS}$ , and  $3YBE^{UHS}$ ), and of a conventionally sintered  $3Y^{CS}$  sample as a reference. The conventionally sintered  $3Y^{CS}$  sample, which attained full density, exhibited no detectable amount of residual chlorine. This provides the conclusion that the residual chlorine in YSZ ceramics is harmless during conventional sintering because all the chlorine volatilizes before the pores are closed. In contrast, a spectrum of a poorly densified  $3Y^{UHS}$  sample exhibited a strong chlorine peak. The poorly densified  $3YE^{UHS}$  sample also displayed a chlorine peak of comparable magnitude. The chlorine peaks measured in  $3YB^{UHS}$  and  $3YBE^{UHS}$  samples were markedly lower, approximately a quarter of the levels observed in  $3Y^{UHS}$  and  $3YE^{UHS}$  samples.

The quantification of the LEIS spectra is generally challenging [15], especially in the case when  $ZrCl_4$  is not homogeneously distributed in sintered 3YSZ. It evaporates from particle surfaces and condenses into the neck area between contacting particles [20], embedding the chlorine atoms at grain boundaries and grain-to-pore interfaces. Nevertheless, we can assume that the poorly densified 3Y and 3YE samples entrapped up to 0.07 wt% of residual chlorine which was the amount of chlorine detected in their as-received state [11] and after heating at 900 °C [12]. The critical amount of residual chlorine which had a measurable negative effect on the densification of 3YSZ was estimated based on several experimental data in our previous study as 0.03 wt% [12]. Therefore, based on our assumption, the poorly densified 3Y and 3YE samples had more than twice the critical amount of residual chlorine, while the almost fully dense 3YB and 3YBE samples had only 0.0175 wt% of chlorine ( $\frac{1}{4}$  of 0.07 wt% in the context of the LEIS results), which is under the critical amount.

The results presented in this study show that the presence of residual

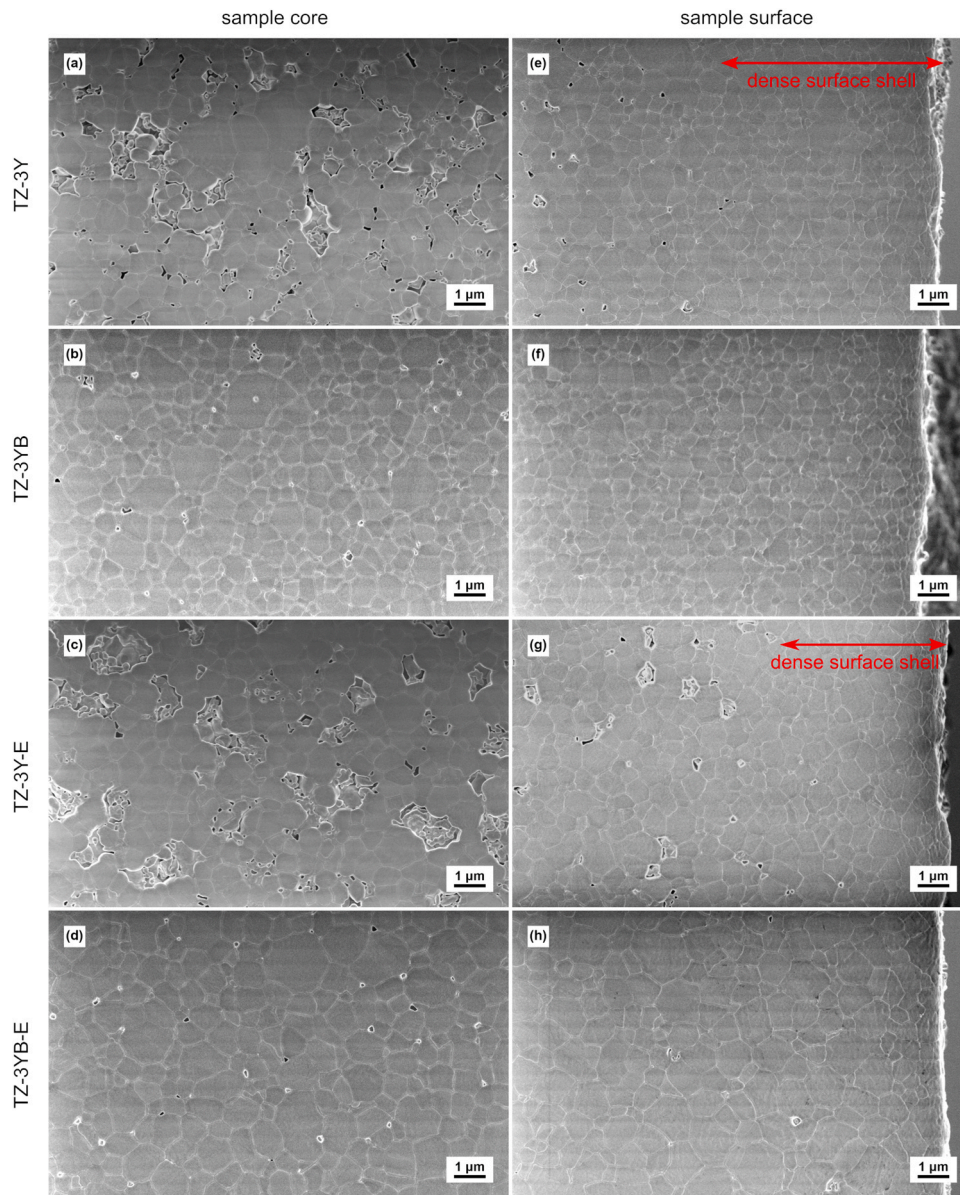


Fig. 3. Microstructure in the core (a-d) and under the surface (e-f) of ultra-fast sintered samples at 1780 °C.

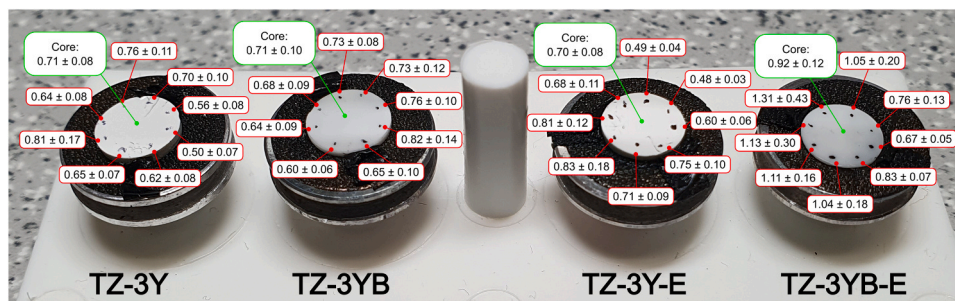


Fig. 4. Average grain size ( $\pm$  standard deviation) in  $\mu\text{m}$  at different sample positions. Samples were ultrafast sintered at 1780 °C. Black dots made with a black marker on the polished surface were used for orientation during SEM imaging.

chlorine in 3YSZ powders is a critical problem for densification during UHS. A solution might be to lower the UHS heating rate into the same magnitude as used during conventional sintering (see [Table S2](#) in [Supplementary Materials](#)), however, this would also reduce the practical

advantage of UHS – rapid densification. Thus, our work underscores an important limitation of current UHS practice: without addressing chlorine entrapment, the full benefits of this method cannot be realized in 3YSZ ceramics. So far, studies on UHS of 3YSZ often used a pre-sintering

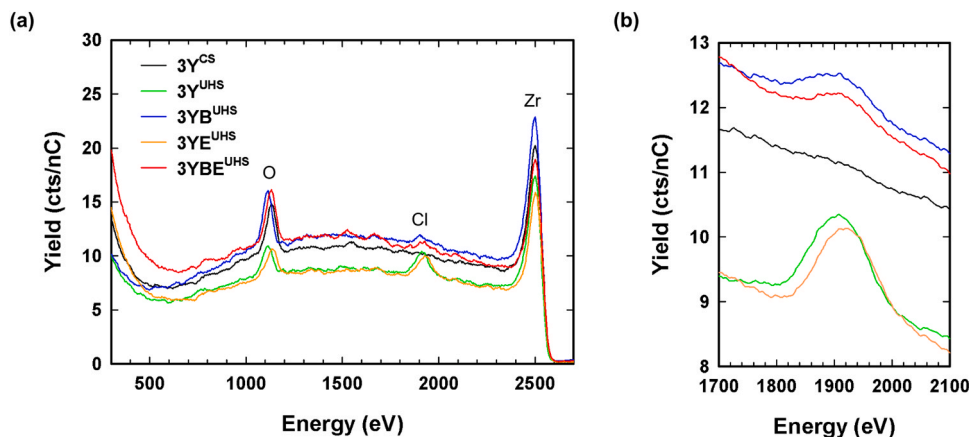


Fig. 5. Low Energy Ion Scattering spectra of ultrafast sintered samples at 1406 °C ( $3Y^{UHS}$ ,  $3YB^{UHS}$ ,  $3YE^{UHS}$ , and  $3YBE^{UHS}$ ) and of a conventionally sintered  $3Y^{CS}$  sample: (a) overview, (b) detail on the chlorine peak.

cycle at 1000 °C for 60 min to obtain a high density and address volatile species [6–8], but our present results indicate that it is not necessary in every case. Some commercially available 3YSZ, for example, binder-containing grades from Tosoh Corp. (TZ-3YB, TZ-3YB-E) minimize the initially higher amount of residual chlorine during binder burnout [11], removing the necessity of the pre-sintering cycle. Alternatively, the UHS should utilize 3YSZ powders synthesised from chlorine-free precursors (alkoxides, nitrates, sulphates, etc.) which would not manifest the negative densification effect of residual chlorine.

#### 4. Conclusions

Recent studies of UHS of 3YSZ ceramics often used pre-sintering of green bodies at 1000 °C for 60 min to remove entrapped gases, which is time and energetically counterproductive. We sintered four commercially available 3YSZ powder grades produced by Tosoh Corp. without this pre-sintering treatment. Two out of four powder grades, without binder, densified poorly (TZ-3Y, TZ-3Y-E specimens) and the other two, with added binder, reached almost full density (TZ-3YB, TZ-3YB-E specimens). We clarified that poor densification of the binderless grades is a result of a residual chlorine entrapment inside the sintered sample due to rapid pore closure caused by the ultrafast heating rate. Trapped residual chlorine then volatilized within the sample core which prevented its further densification. The presence of residual chlorine in sintered specimens was analysed by the surface-sensitive Low Energy Ion Scattering (LEIS) technique which showed that the amount of residual chlorine in poorly densified samples was about four times as much as in the samples that achieved nearly full density. The presence of binder evidently enables the removal of chlorine during burnout at lower temperatures, but the details of the chemistry involved remain to be elucidated.

#### CRedit authorship contribution statement

**Vladimír Prajzler:** Writing – review & editing, Writing – original draft, Visualization, Resources, Project administration, Methodology, Investigation, Funding acquisition, Conceptualization. **Zonghao Guo:** Writing – review & editing, Visualization, Investigation. **Stanislav Průša:** Writing – review & editing, Visualization, Investigation. **Richard I. Todd:** Writing – review & editing, Supervision, Resources, Funding acquisition.

#### Declaration of Competing Interest

The authors declare that they have no known competing financial interests or personal relationships that could have appeared to influence

the work reported in this paper.

#### Acknowledgements

The research was funded by the Czech Science Foundation (GAČR), project No. 22-30487O. Additionally, this publication was supported by the project “Mechanical Engineering and Bio-inspired Systems”, funded as project No. CZ.02.01.01/00/22\_008/ 0004634 by Programme Johannes Amos Comenius, call Excellent Research. Czech-NanoLab project LM2023051 funded by MEYS CR is gratefully acknowledged for the financial support of the measurements/sample fabrication at CEITEC Nano Research Infrastructure.

#### Appendix A. Supporting information

Supplementary data associated with this article can be found in the online version at [doi:10.1016/j.jeurceramsoc.2025.117709](https://doi.org/10.1016/j.jeurceramsoc.2025.117709).

#### Data Availability

The datasets generated and/or analysed during the current study are available in the repository under following DOI: [10.5281/zenodo.15340519](https://doi.org/10.5281/zenodo.15340519).

#### References

- [1] M. Biesuz, S. Grasso, V.M. Sglavo, What's new in ceramics sintering? a short report on the latest trends and future prospects, *Curr. Opin. Solid State Mater. Sci.* 24 (2020) 100868.
- [2] D. Kim, C.H. Kim, Effect of heating rate on pore shrinkage in yttria-doped zirconia, *J. Am. Ceram. Soc.* 76 (1993) 1877–1878.
- [3] W. Ji, J. Zhang, W. Wang, Z. Fu, R.I. Todd, The microstructural origin of rapid densification in 3YSZ during ultra-fast firing with or without an electric field, *J. Eur. Ceram. Soc.* 40 (2020) 5829–5836.
- [4] M. Biesuz, T.H. de Beauvoir, E. De Bona, M. Cassetta, C. Manière, V.M. Sglavo, C. Estournès, Ultrafast high-temperature sintering (UHS) vs. conventional sintering of 3YSZ: microstructure and properties, *J. Eur. Ceram. Soc.* 44 (2024) 4741–4750.
- [5] C. Wang, W. Ping, Q. Bai, H. Cui, R. Hensleigh, R. Wang, A.H. Brozena, Z. Xu, J. Dai, Y. Pei, C. Zheng, G. Pastel, J. Gao, X. Wang, H. Wang, J.-C. Zhao, B. Yang, X. (Rayne) Zheng, J. Luo, Y. Mo, B. Dunn, L. Hu, A general method to synthesize and sinter bulk ceramics in seconds, *Science* 368 (2020) 521–526.
- [6] J. Dong, V. Pouchly, M. Biesuz, V. Tyrpekl, M. Vilémová, M. Kermani, M. Reece, C. Hu, S. Grasso, Thermally-insulated ultra-fast high temperature sintering (UHS) of zirconia: a master sintering curve analysis, *Scr. Mater.* 203 (2021) 114076.
- [7] J. Wu, M. Kermani, D. Zhu, J. Li, Y. Lin, C. Hu, S. Grasso, Carbon free ultra-fast high temperature sintering of translucent zirconia, *Scr. Mater.* 210 (2022) 114476.
- [8] S. Wang, T.P. Mishra, Y. Deng, L. Balice, A. Kaletsch, M. Bram, C. Broeckmann, Electric current-assisted sintering of 8YSZ: a comparative study of ultrafast high-temperature sintering and flash sintering, *Adv. Eng. Mater.* 25 (2023).
- [9] D. Kim, C.H. Kim, Entrapped gas effect in the fast firing of yttria-doped zirconia, *J. Am. Ceram. Soc.* 75 (1992) 716–718.
- [10] S. Sweeney, M. Mayo, Origin of unusual sintering phenomena in compacts of chloride-derived 3Y-TZP nanopowders, *Sci. Sinter.* 46 (2014) 169–184.

- [11] V. Prajzler, S. Průša, K. Maca, Rapid pressure-less sintering of fine grained zirconia ceramics: Explanation and elimination of a core-shell structure, *J. Eur. Ceram. Soc.* 39 (2019) 5309–5319.
- [12] V. Prajzler, K. Maca, R. Todd, Residual chlorine prevents full densification of flash sintered yttria-stabilized zirconia ceramics, *J. Eur. Ceram. Soc.* 44 (2024) 6660–6667.
- [13] Z.H. Guo, R.I. Todd, Acceleration of grain boundary diffusion during ultra-fast firing (UHS) of alumina powder compacts, *Acta Mater.* 282 (2025) 120471.
- [14] M.I. Mendelson, Average grain size in polycrystalline ceramics, *J. Am. Ceram. Soc.* 52 (1969) 443–446.
- [15] S. Průša, M.R. Linford, E. Vanfěková, P. Bábík, J.W. Pinder, T. Šikola, H. H. Brongersma, A practical guide to interpreting low energy ion scattering (LEIS) spectra, *Appl. Surf. Sci.* 652 (2024) 158793.
- [16] K. Matsui, N. Ohmichi, M. Ohgai, N. Enomoto, J. Hojo, Sintering kinetics at constant rates of heating: effect of Al<sub>2</sub>O<sub>3</sub> on the initial sintering stage of fine zirconia powder, *J. Am. Ceram. Soc.* 88 (2005) 3346–3352.
- [17] T.P. Mishra, S. Wang, C. Lenser, D. Jennings, M. Kindelmann, W. Rheinheimer, C. Broeckmann, M. Bram, O. Guillon, Ultra-fast high-temperature sintering of strontium titanate, *Acta Mater.* 231 (2022) 117918.
- [18] M.J. Mayo, Processing of nanocrystalline ceramics from ultrafine particles, *Int. Mater. Rev.* 41 (1996) 85–114.
- [19] M. Valigi, A. Cimino, D. Gazzoli, G. Minelli, The influence of additives (Cl<sup>-</sup>, ReO<sub>4</sub><sup>-</sup>, Ti(IV)) on some properties of ZrO<sub>2</sub>, *Solid State Ion.* 32/33 (1989) 698–705.
- [20] M.J. Readey, D.W. Readey, Sintering of ZrO<sub>2</sub> in HCl atmospheres, *J. Am. Ceram. Soc.* 69 (1986) 580–582.